

Even parity excitations of the nucleon in lattice QCD

B. G. Lasscock,¹ J. N. Hedditch,¹ W. Kamleh,¹ D. B. Leinweber,¹
W. Melnitchouk,² A. G. Williams,¹ and J. M. Zanotti³

¹ *Special Research Centre for the Subatomic Structure of Matter,
and Department of Physics, University of Adelaide, Adelaide SA 5005, Australia*

² *Jefferson Lab, 12000 Jefferson Avenue, Newport News, VA 23606, USA*

³ *School of Physics, University of Edinburgh, Edinburgh EH9 3JZ, UK*

We study the spectrum of the even parity excitations of the nucleon in quenched lattice QCD. We extend our earlier analysis by including an expanded basis of nucleon interpolating fields, increasing the physical size of the lattice, including more configurations to enhance statistics and probing closer to the chiral limit. With a review of world lattice data, we conclude that there is little evidence of the Roper resonance in quenched lattice QCD.

PACS numbers: 11.15.Ha, 12.38.Gc, 12.38.Aw

Keywords:

I. INTRODUCTION

One of the long-standing puzzles in baryon spectroscopy has been the low mass of the first positive parity excitation of the nucleon, the $J^P = \frac{1}{2}^+$ Roper resonance, or $N^*(1440)$. In constituent (or valence) quark models with harmonic oscillator quark-quark potentials, the lowest-lying odd parity ($J^P = \frac{1}{2}^-$) state naturally occurs below the positive parity radial excitation (with principal quantum number $N = 2$), whereas in nature the Roper resonance is almost 100 MeV below the $\frac{1}{2}^- N^*(1535)$ state. Without fine tuning of parameters, valence quark models tend to leave the mass of the Roper resonance too high.

Over the years various suggestions have been made to explain this anomaly, ranging from speculations that the Roper resonance may be a hybrid baryon state with excited glue [1, 2], or a meson-baryon system [3], or in terms of “breathing modes” of the ground state nucleon [4]. To understand the nature of the Roper resonance in the context of QCD, a number of studies have been performed recently within lattice QCD.

The study of excited baryons on the lattice has had a relatively short history, although recently there has been growing interest in identifying new techniques to isolate excited baryons, motivated partly by the experimental N^* program at Jefferson Lab. The first detailed analysis of the positive parity excitation of the nucleon was performed by Leinweber [5] using Wilson fermions and an operator product expansion spectral ansatz.

In previous work by the CSSM Lattice Collaboration [6] an analysis of the spectrum of octet baryons was performed using the FLIC fermion action. In each channel, a 2×2 correlation matrix was used to extract the low-lying states. This approach was found to be successful in extracting the first excited state of the negative parity $N^*(1535)$ state, and in the analysis of the Λ interpolating field. However, the identification of the Roper resonance with this correlation matrix remained elusive.

In the present study we extend the earlier work in sev-

eral directions, while focusing on the even parity nucleon spectrum. In addition, we work with a larger lattice volume (2.5 fm compared to 1.95 fm in Refs. [6, 7]), reducing finite volume effects and enhancing the statistics. Most importantly, we also use an expanded basis of interpolators compared with that in Ref. [6], with the addition of the spin-1/2 projected nucleon interpolator used in the calculation of the spin-3/2 hadron mass spectrum [7].

In the even parity spin-1/2 nucleon channel it is well known that the two standard interpolating fields, which we label χ_1 and χ_2 , individually access the ground state and an excited state, respectively. The application of a 2×2 correlation matrix with these interpolators finds no evidence of a state with a mass different from those that can already be extracted with the two interpolators individually [6]. Furthermore, the extracted excited state is found to be too massive to be identified with the Roper resonance, and is therefore more likely to have stronger overlap with the next even parity excited state of the nucleon with mass 1710 MeV — which we denote by $N'(1710)$ (in general we label even parity nucleon excitations on the lattice by a superscript “ ’ ”, and odd parity excitations on the lattice by a superscript “ * ”). These findings are consistent with a similar correlation matrix analysis by Sasaki et al. [8].

At the larger quark masses typically used in lattice calculations of the spectrum, we expect that the three lowest-lying spin-1/2 even parity states are the ground state nucleon, the Roper, and the second even parity excited state (the $N'(1710)$), the latter which appears to have strong coupling to the χ_2 interpolator. One would therefore naïvely expect that the addition of a third nucleon interpolator to our basis should allow the mass of the Roper to be extracted (in quenched lattice QCD). In Ref. [7] the spectra of the nucleon and Δ were analysed, including both spin-1/2 and spin-3/2 excited states. For the nucleon spectrum a mixed spin-1/2, spin-3/2 interpolating field (labeled χ_3) was used. The spin-1/2 projected χ_3 interpolator was found to have good overlap with the ground state, and in the present work we use this interpolator as the third interpolating field.

In a similar analysis, Brömmel et al. [9] used the χ_1 and χ_2 interpolators with the time-component of the χ_3 interpolator as a basis for a 3×3 correlation matrix analysis. Even with the larger basis, Brömmel et al. do not identify the Roper on the lattice. The difference between that study [9] and our present analysis is that we consider the spatial components of the χ_3 interpolator, with spin-1/2 projection as in Ref. [7].

In Sec. II we review existing lattice calculations of the positive parity excited nucleon spectrum and attempts to identify the Roper resonance on the lattice. Our lattice techniques are outlined in Sec. III, where we firstly summarise our simulation parameters and interpolating fields. This is followed by a discussion of how to identify the spinor indices in which the odd and even parity contributions to the correlation functions propagate. Our results are reported in Sec. IV, and conclusions summarised in Sec. V.

II. EXISTING LATTICE RESULTS

In this section we review the findings of earlier lattice studies of the spin-1/2, even parity nucleon mass spectrum. Figure 1 shows a compilation of recent calculations of the mass spectrum in quenched lattice QCD. Because the masses of the excited states at small lattice volumes are expected to suffer from significant finite volume effects, we focus only on those results obtained on lattices with a physical size ≥ 2.0 fm.

In Fig. 1 the studies using Bayesian techniques — namely, Sasaki et al. [11] (pluses) and Mathur et al. [12] (crosses) — identify an excited state which is interpreted as the Roper resonance. The physical size of the lattice in these analyses is 3.0 fm and 3.2 fm, respectively, and both use point sources. In both studies the mass of the odd parity excited state is found to be consistent with that of the empirical $N^*(1535)$ resonance. At large quark masses, the level ordering of the even and odd parity excited states is reversed compared to the physical level ordering. However, at small quark masses (m_π as small as 180 MeV) Mathur et al. [12] find that the correct empirical ordering appears to be restored. However it is suggested by Mathur et al. that greater statistics are required to determine if this is true.

The masses in Fig. 1 which are extracted using a correlation matrix include the previous study by the CSSM Lattice Collaboration [6] (open circles), Brömmel et al. [9] (squares), Burch et al. [13] (triangles), and Basak et al. [10] (diamonds). The mass of the excited state extracted with a 3×3 correlation matrix in the present analysis is also shown (filled circles).

The previous CSSM work [6] used the χ_1 and χ_2 interpolators as a basis in the correlation, with a physical lattice size of 1.92 fm. At the fermion source 20 sweeps of gauge invariant Gaussian smearing were used, with a smearing fraction of 0.7. The findings strongly suggest that the mass of the extracted excited state is too large

to be identified with the Roper resonance. These results sit somewhat high because of the relatively small volume employed in the analysis.

A larger basis of operators is considered by Burch et al. in Ref. [13]. That study considers χ_1 , χ_2 and an interpolator equivalent to the temporal component of χ_3 (up to an overall factor of γ_0). To expand the operator basis, two different fermion source and sink Jacobi smearing prescriptions, labeled “wide” and “narrow”, are considered for each quark. The narrow sources have 18 sweeps of smearing with a smearing fraction of $\kappa = 0.210$, while the wide sources have 41 sweeps with $\kappa = 0.191$. The physical size of the lattice is 2.38 fm. In the analysis of Ref. [13] the basis of operators is restricted to χ_1 and the χ_3 -like interpolator with three different smearing prescriptions for each interpolator, making a total of six different operators.

In Refs. [13] and [14] Burch et al. argue that in the limit of large quark mass, the state corresponding to the N' can be identified by comparison with the mass extracted with the χ_2 interpolator. They consequently identify the largest mass state with the N' and conclude that the lower energy state is therefore the Roper. We note that at the larger quark masses the lower energy state, identified as the Roper with the Bayesian techniques in Ref. [12], is similar to the mass of the same state identified using a correlation matrix analysis in Ref. [13]. However, the two techniques disagree at the smaller quark masses.

Basak et al. [10] take advantage of the discrete symmetries on the lattice and identify a large basis of local and non-local operators [15]. The complete set of local and singly displaced non-local sources are used as a basis of their correlation matrix, and two distinct excited states are identified. The interpretation of Basak et al. [10] is that the lower energy excited state corresponds to the N' . This state is consistent with the higher energy state found by Burch et al. [13], and our new results presented herein.

The best fit to the excited state data extracted on a lattice with physical size ~ 2.5 fm using the correlation matrix technique is shown by the solid line in Fig. 1. We fit the data for the largest energy state extracted by Burch et al. [13], along with the data from Basak et al. [10] and Brömmel et al. [9], and the results of the present study. Our results are consistent with the masses extracted by Brömmel et al. and by Burch et al. at their largest quark masses. At the smaller quark masses, the highest mass states obtained by Burch et al. and Basak et al. lie on either side of the line of best fit. Since these two analyses use different gauge and quark actions, it is not possible to determine whether the small discrepancy between their masses is of any statistical significance. It is also likely that the operators considered in each study have different couplings to the $N + \pi$ in P-wave (and equivalently the P-wave $N + \eta'$ in quenched QCD) scattering state. We know that as smaller quark masses are approached, the level ordering between the lowest energy

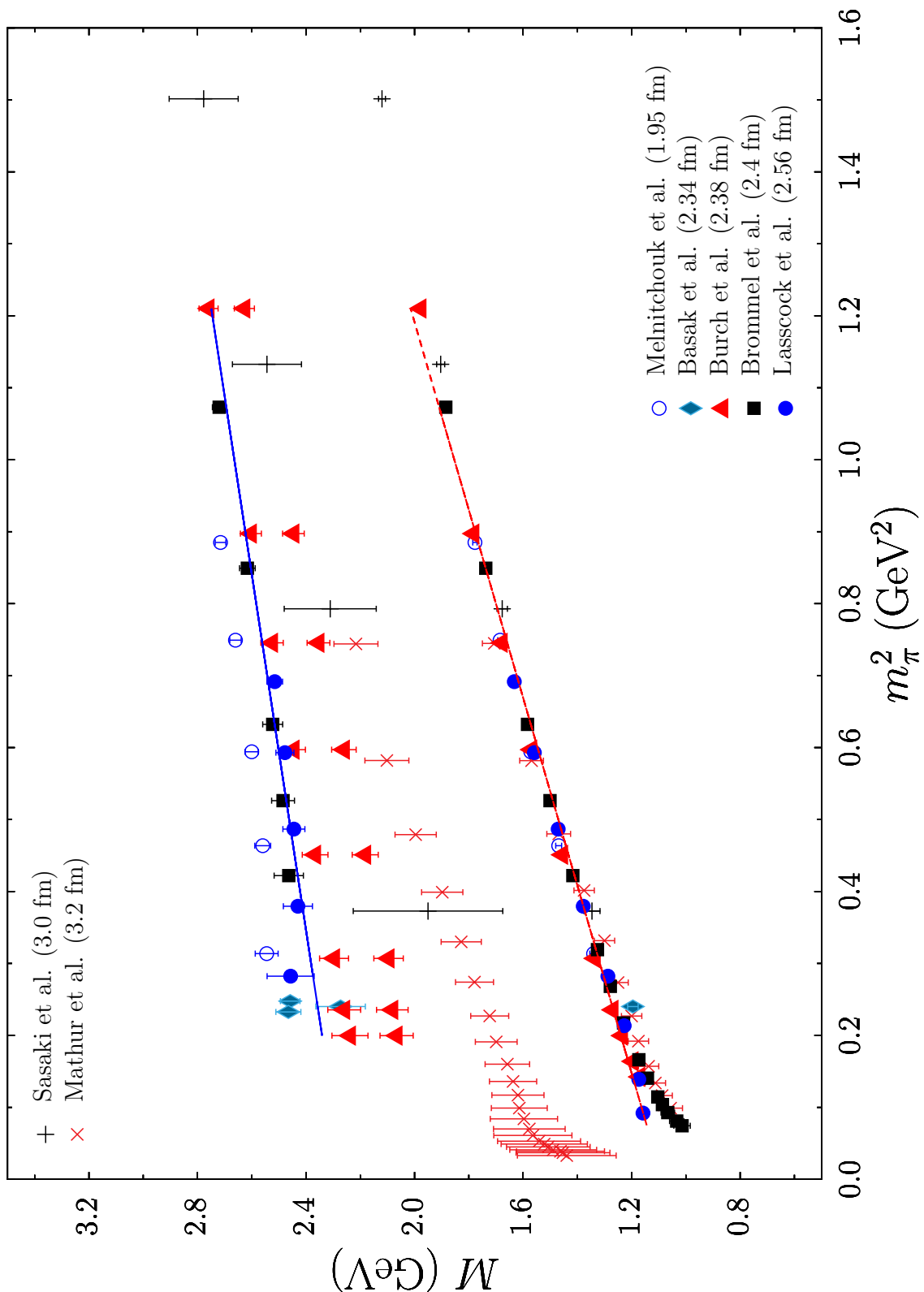


FIG. 1: Compilation of current lattice calculations of the spectrum of the even parity spin-1/2 excited states of the nucleon. In each study the ground state and excited state masses are shown. Burch et al. (closed triangles) report two excited states, one as the N' the other as a Roper candidate. Basak et al. (diamonds) report the masses of three excited states. Note that the two data points with degenerate masses from Basak et al. [10] have been displaced horizontally for clarity. To aid in understanding the results, lines of best fit to the N' and ground state masses are included. The solid line is a line of best fit to the N' excited state masses extracted in this study, and the studies of Basak et al. , Burch et al. and Brommel et al. . The dashed line is a line of best fit to the ground state mass for all of the data shown.

multi-hadron state and the N' state is reversed on the lattice.

III. LATTICE TECHNIQUES

The present analysis is based on an ensemble of 396 gauge-field configurations on a $20^3 \times 40$ lattice, using the mean-field $\mathcal{O}(a^2)$ -improved Luscher-Weisz plaquette plus rectangle gauge action [16]. The lattice spacing is 0.128 fm, set with the Sommer scale $r_0 = 0.49$ fm. For the fermion propagators we use the FLIC fermion action [17], which is an $\mathcal{O}(a)$ -improved action with excellent scaling properties, providing near continuum results at finite lattice spacing [18]. A fixed boundary condition in the time direction is implemented by setting $U_t(\vec{x}, N_t) = 0 \forall \vec{x}$ in the hopping terms of the fermion action. Periodic boundary conditions are imposed in the spatial directions. We find that the fixed boundary effects are only significant after time slice 30 [19], which is the limit of our analysis of the correlation functions presented below.

We apply 36 sweeps of gauge-invariant Gaussian smearing [20], with smearing fraction $\alpha = 0.7$, in the spatial dimensions at the fermion source ($t = 8$). Eight quark masses are considered in this calculation, providing $am_\pi = \{ 0.540, 0.500, 0.453, 0.400, 0.345, 0.300, 0.242, 0.197 \}$. The error analysis is performed by a second-order, single-elimination jackknife, with the χ^2 per degree of freedom obtained via covariance matrix fits. Further details of the fermion action and simulation parameters can be found in Refs. [17, 18] and [19, 21], respectively. We apply the variational method as discussed in Refs. [6, 21].

A. Interpolating Fields

In the previous CSSM study [6] the χ_1 and χ_2 interpolators were found not to have significant overlap with

each other. Following the approach by Brömmel et al. [9], we extend this analysis by including the χ_3 interpolator that was used by Zanotti et al. [7] to extract spin-3/2 nucleon excited states. Our basis of nucleon interpolating fields is then given by:

$$\begin{aligned}\chi_1(x) &= \epsilon^{abc}(u^{Ta}(x)C\gamma_5 d^b(x))u^c(x), \\ \chi_2(x) &= \epsilon^{abc}(u^{Ta}(x)Cd^b(x))\gamma_5 u^c(x), \\ \chi_3^\mu(x) &= \epsilon^{abc}(u^{Ta}(x)C\gamma_5\gamma^\mu d^b(x))\gamma_5 u^c(x).\end{aligned}\quad (1)$$

In all of our phenomenology we use the Dirac representation of the γ -matrices.

B. Excited baryons on the lattice

We begin our discussion with a review of how the masses of even and odd parity states are extracted from the correlation function using the spin-1/2 χ_1 and χ_2 interpolators. On the baryon level, the two-point correlation function in momentum space is:

$$\mathcal{G}(t, \vec{p}) = \sum_{\vec{x}} e^{-i\vec{p}\cdot\vec{x}} \langle 0 | T \chi(x) \bar{\chi}(0) | 0 \rangle, \quad (2)$$

where the interpolator $\chi(\vec{x})$ annihilates (creates) baryon states to (from) the vacuum. Inserting a complete set of intermediate momentum, energy and spin states $|B, \vec{p}', s\rangle$,

$$1 = \sum_{B, \vec{p}', s} |B, \vec{p}', s\rangle \langle B, \vec{p}', s|, \quad (3)$$

we obtain

$$\mathcal{G}(t, \vec{p}) = \sum_{s, \vec{p}', B} \sum_{\vec{x}} e^{-i\vec{p}\cdot\vec{x}} \langle 0 | \chi(x) |B, \vec{p}', s\rangle \langle B, \vec{p}', s | \bar{\chi}(0) | 0 \rangle, \quad (4)$$

where the state B has mass M_B and energy $E_B = \sqrt{M_B^2 + \vec{p}^2}$. The sum over all possible states B with a given set of quantum numbers includes a tower of resonances and multi-hadron states created by our interpolators. Using $\chi(x) = e^{iP\cdot x} \chi(0) e^{-iP\cdot x}$, where P is the four-momentum operator, we can write:

$$\begin{aligned}\mathcal{G}(t, \vec{p}) &= \sum_{s, \vec{p}', B} \sum_{\vec{x}} e^{-i\vec{p}\cdot\vec{x}} \langle 0 | e^{iP\cdot x} \chi(0) e^{-iP\cdot x} |B, \vec{p}', s\rangle \langle B, \vec{p}', s | \bar{\chi}(0) | 0 \rangle \\ &= \sum_{s, \vec{p}', B} e^{-iE_B t} \sum_{\vec{x}} e^{-i\vec{x}\cdot(\vec{p}-\vec{p}')} \langle 0 | \chi(0) |B, \vec{p}', s\rangle \langle B, \vec{p}', s | \bar{\chi}(0) | 0 \rangle \\ &= \sum_{s, \vec{p}', B} e^{-iE_B t} \delta_{\vec{p}\vec{p}'} \langle 0 | \chi(0) |B, \vec{p}', s\rangle \langle B, \vec{p}', s | \bar{\chi}(0) | 0 \rangle \\ &\rightarrow \sum_B e^{-E_B t} \sum_s \langle 0 | \chi(0) |B, \vec{p}, s\rangle \langle B, \vec{p}, s | \bar{\chi}(0) | 0 \rangle,\end{aligned}\quad (5)$$

where on the last line we make the replacement $it \rightarrow t$ for Euclidean time.

Next we evaluate the matrix elements in Eq. (5), labeling the even and odd parity contributions to the correlation function by “+” and “-”, respectively. The overlap of χ and $\bar{\chi}$ with even and odd parity baryons, such as the nucleon for example, can be expressed as:

$$\begin{aligned}
\langle 0 | \chi(0) | N_{1/2+}(\vec{p}, s) \rangle &= \lambda_{N_{1/2+}} \sqrt{\frac{M_{N_{1/2+}}}{E_{N_{1/2+}}}} u(p_{N_{1/2+}}, s) , \\
\langle 0 | \chi(0) | N_{1/2-}(\vec{p}, s) \rangle &= \lambda_{N_{1/2-}} \sqrt{\frac{M_{N_{1/2-}}}{E_{N_{1/2-}}}} \gamma_5 u(p_{N_{1/2-}}, s) , \\
\langle N_{1/2+}(\vec{p}, s) | \bar{\chi}(0) | 0 \rangle &= \bar{\lambda}_{N_{1/2+}} \sqrt{\frac{M_{N_{1/2+}}}{E_{N_{1/2+}}}} \bar{u}(p_{N_{1/2+}}, s) , \\
\langle N_{1/2-}(\vec{p}, s) | \bar{\chi}(0) | 0 \rangle &= -\bar{\lambda}_{N_{1/2-}} \sqrt{\frac{M_{N_{1/2-}}}{E_{N_{1/2-}}}} \bar{u}(p_{N_{1/2-}}, s) \gamma_5 ,
\end{aligned} \tag{6}$$

where $u(p, s)$ is a Dirac spinor and $\lambda(\bar{\lambda})$ are couplings of the interpolators at the sink (source). Note that the four-momentum $p_{N_{1/2+}}$ is on-shell, with $p_0 = \sqrt{\vec{p}^2 + M_{N_{1/2+}}^2}$. Because the fermion source is smeared, the coupling $\bar{\lambda}$ is not equal to the adjoint of λ .

Substituting the appropriate terms and using the identity

$$\sum_s u(p, s) \bar{u}(p, s) = \frac{(\gamma \cdot p + M)}{2M} , \tag{7}$$

the contributions of the even and odd parity terms to the correlation function can be written as:

$$\begin{aligned}
\mathcal{G}(t, \vec{p}) &= \sum_{B^+} \lambda_{B^+} \bar{\lambda}_{B^+} e^{-E_{B^+} t} \frac{(\gamma \cdot p_{B^+} + M_{B^+})}{2E_{B^+}} \\
&+ \sum_{B^-} \lambda_{B^-} \bar{\lambda}_{B^-} e^{-E_{B^-} t} \frac{(\gamma \cdot p_{B^-} - M_{B^-})}{2E_{B^-}} .
\end{aligned} \tag{8}$$

The masses of states with definite parity can then be obtained from the spinor trace of the parity projected

correlation functions,

$$\begin{aligned}
G_{\pm}(t, \vec{0}) &= \text{tr}_{\text{sp}} \left[\Gamma_{\pm} \mathcal{G}(t, \vec{0}) \right] \\
&= \sum_{B^{\pm}} \lambda_{B^{\pm}} \bar{\lambda}_{B^{\pm}} \exp(-E_{B^{\pm}} t) \\
&\stackrel{t \rightarrow \infty}{=} \lambda_{0^{\pm}} \bar{\lambda}_{0^{\pm}} \exp(-M_{0^{\pm}} t) ,
\end{aligned} \tag{9}$$

where $\Gamma_{\pm} = \frac{\gamma_0 \pm 1}{2}$ is the parity projection operator at zero momentum [22], and the subscripts 0^{\pm} label the lowest energy state with the projected quantum numbers.

For the χ_3^{μ} interpolator the analogue of Eq. (5) is given by:

$$P^{\mu\nu}(t, \vec{p}) = \sum_B e^{-E_B t} \sum_s \langle 0 | \chi_3^{\mu}(0) | B, \vec{p}, s \rangle \langle B, \vec{p}, s | \bar{\chi}_3^{\nu}(0) | 0 \rangle , \tag{10}$$

where now χ_3^{μ} overlaps with both spin-1/2 and spin-3/2 states. In this study we project spin-1/2 states using the spin projection operator discussed in Ref. [7],

$$P_{\mu\nu}^{\frac{1}{2}}(p) = \frac{1}{3} \gamma_{\mu} \gamma_{\nu} + \frac{1}{3p^2} (\gamma \cdot p \gamma_{\mu} p_{\nu} + p_{\mu} \gamma_{\nu} \gamma \cdot p) . \tag{11}$$

At zero momentum $p = (M, 0, 0, 0)$, relevant to the mass determination, the spin-projection operator has no hypercubic lattice artifacts.

We proceed in our analysis of the χ_3^{μ} interpolator by evaluating the analogue of the matrix element in Eqs. (6). Following Zanotti et al. [7], the coefficient of the spinor is taken to be a linear combination of four-vectors. The requirement that the matrix elements transform as pseudovectors under parity restricts the coefficients to be proportional

to either the four-momentum or the matrix γ^μ . The analogue of Eqs. (6) can therefore be written as:

$$\langle 0|\chi_3^\mu(0)|N_{1/2^+}(\vec{p}, s)\rangle = (\alpha_{N_{1/2^+}} p_{N_{1/2^+}}^\mu + \beta_{N_{1/2^+}} \gamma^\mu) \sqrt{\frac{M_{N_{1/2^+}}}{E_{N_{1/2^+}}}} \gamma_5 u(p_{N_{1/2^+}}, s), \quad (12)$$

$$\langle 0|\chi_3^\mu(0)|N_{1/2^-}(\vec{p}, s)\rangle = (\alpha_{N_{1/2^-}} p_{N_{1/2^-}}^\mu + \beta_{N_{1/2^-}} \gamma^\mu) \sqrt{\frac{M_{N_{1/2^-}}}{E_{N_{1/2^-}}}} u(p_{N_{1/2^-}}, s), \quad (13)$$

$$\langle N_{1/2^+}(\vec{p}, s)|\bar{\chi}_3^\mu(0)|0\rangle = -\sqrt{\frac{M_{N_{1/2^+}}}{E_{N_{1/2^+}}}} \bar{u}(p_{N_{1/2^+}}, s) \gamma_5 (\bar{\alpha}_{N_{1/2^+}} p_{N_{1/2^+}}^\mu + \bar{\beta}_{N_{1/2^+}} \gamma^\mu), \quad (14)$$

$$\langle N_{1/2^-}(\vec{p}, s)|\bar{\chi}_3^\mu(0)|0\rangle = \sqrt{\frac{M_{N_{1/2^-}}}{E_{N_{1/2^-}}}} \bar{u}(p_{N_{1/2^-}}, s) (\bar{\alpha}_{N_{1/2^-}} p_{N_{1/2^-}}^\mu + \bar{\beta}_{N_{1/2^-}} \gamma^\mu), \quad (15)$$

where the factors α_B and β_B denote the coupling strengths of the interpolating field χ_3^μ to the baryon B , and similarly for the adjoint. Combining these expressions with their respective adjoints, and using Eq. (7) for the energy projector, the contribution to the correlation function from spin-1/2 states extracted with χ_3^μ is:

$$\begin{aligned} \mathcal{G}(t, \vec{p}) &= \sum_{B^+} e^{-E_B t} (\alpha_{N_{1/2^+}} p_{N_{1/2^+}}^\nu + \beta_{N_{1/2^+}} \gamma^\nu) \gamma_5 \frac{\gamma \cdot p_{N_{1/2^+}} + M_{N_{1/2^+}}}{2E_{N_{1/2^+}}} \gamma_5 (\bar{\alpha}_{N_{1/2^+}} p_{N_{1/2^+}}^\nu + \bar{\beta}_{N_{1/2^+}} \gamma^\nu) \\ &+ \sum_{B^-} e^{-E_B t} (\alpha_{N_{1/2^-}} p_{N_{1/2^-}}^\nu + \beta_{N_{1/2^-}} \gamma^\nu) \frac{\gamma \cdot p_{N_{1/2^-}} + M_{N_{1/2^-}}}{2E_{N_{1/2^-}}} (\bar{\alpha}_{N_{1/2^-}} p_{N_{1/2^-}}^\nu + \bar{\beta}_{N_{1/2^-}} \gamma^\nu). \end{aligned} \quad (16)$$

In this analysis we average over the contributions to the spin-projected correlation function with $\mu = 1-3$ and $\nu = 1-3$. We need not evaluate the $(\mu, \nu) = (k, 0)$ or $(0, k)$ terms, where $k = 1-3$, as these do not contribute to the correlation function after spin projection at $\vec{p} = \vec{0}$.

Finally, we evaluate the two-point function at the hadronic level for the cross correlators $\langle 0|T\chi_3^\mu \bar{\chi}_i|0\rangle$ and $\langle 0|T\chi_i \bar{\chi}_3^\mu|0\rangle$, with $i = 1, 2$. It is important to note that as these correlation functions are not Lorentz scalars they remain dependent on the representation of the γ -matrices. The respective correlation functions are given by:

$$\mathcal{G}_{3i}^\mu(t, \vec{p}) = \sum_{\vec{x}} \exp(-i\vec{p} \cdot \vec{x}) \langle 0|T \chi_3^\mu(x) \bar{\chi}_i(0) |0\rangle, \quad (17)$$

$$\mathcal{G}_{i3}^\mu(t, \vec{p}) = \sum_{\vec{x}} \exp(-i\vec{p} \cdot \vec{x}) \langle 0|T \chi_i(x) \bar{\chi}_3^\mu(0) |0\rangle. \quad (18)$$

As for the diagonal correlators discussed above, we proceed by inserting a complete set of states and evaluating the resulting matrix elements. For the function \mathcal{G}_{i3}^μ , we can use Eqs. (6), (7) and (12) to write the matrix elements as:

$$\begin{aligned} &\sum_s \langle 0|\chi_3^\mu(0)|N_{1/2^+}(\vec{p}, s)\rangle \langle N_{1/2^+}(\vec{p}, s)|\bar{\chi}_i(0)|0\rangle \\ &= \bar{\lambda}_{N_{1/2^+}} (\alpha_{N_{1/2^+}} p_{N_{1/2^+}}^\mu + \beta_{N_{1/2^+}} \gamma^\mu) \gamma_5 \frac{(\gamma \cdot p_{N_{1/2^+}} + M_{N_{1/2^+}})}{2E_{N_{1/2^+}}}. \end{aligned} \quad (19)$$

At $\vec{p} = \vec{0}$, the positive parity states for $\mu = 1$ propagate in the real part of the (1, 2) and (2, 1) spinor elements of the correlation function. For $\mu = 2$, the positive parity states propagate in the imaginary part of the (1, 2) and (2, 1) elements, with a relative minus sign. For $\mu = 3$ the positive parity states propagate in the real part of the (1, 1) and (2, 2) elements, with a relative minus sign, and for $\mu = 0$ they propagate in the real part of the (1, 3) and (2, 4) elements.

Similarly, the odd parity contribution to the correlation function is:

$$\begin{aligned} &\sum_s \langle 0|\chi_3^\mu(0)|N_{1/2^-}(\vec{p}, s)\rangle \langle N_{1/2^-}(\vec{p}, s)|\bar{\chi}_i(0)|0\rangle \\ &= \bar{\lambda}_{N_{1/2^-}} (\alpha_{N_{1/2^-}} p_{N_{1/2^-}}^\mu + \beta_{N_{1/2^-}} \gamma^\mu) \gamma_5 \frac{(\gamma \cdot p_{N_{1/2^-}} - M_{N_{1/2^-}})}{2E_{N_{1/2^-}}}. \end{aligned} \quad (20)$$

Combining the even and odd parity contributions, we obtain for the “3*i*” correlation function:

$$\mathcal{G}_{3i}^\mu(t, \vec{p}) = \sum_{B^+} e^{-E_B t} \bar{\lambda}_{N_{1/2^+}} (\alpha_{N_{1/2^+}} p_{N_{1/2^+}}^\mu + \beta_{N_{1/2^+}} \gamma^\mu) \gamma_5 \frac{(\gamma \cdot p_{N_{1/2^+}} + M_{N_{1/2^+}})}{2E_{N_{1/2^+}}}$$

$$+ \sum_{B^-} e^{-E_B t} \bar{\lambda}_{N_{1/2}^-} (\alpha_{N_{1/2}^-} p_{N_{1/2}^-}^\mu + \beta_{N_{1/2}^-} \gamma^\mu) \gamma_5 \frac{(\gamma \cdot p_{N_{1/2}^-} - M_{N_{1/2}^-})}{2E_{N_{1/2}^-}}. \quad (21)$$

Using the appropriate terms in Eqs. (6) and (12) in Eq. (18), the “i3” correlation function can be written:

$$\begin{aligned} \mathcal{G}_{i3}^\mu(t, \vec{p}) &= - \sum_{B^+} e^{-E_B t} \lambda_{N_{1/2}^+} \frac{(\gamma \cdot p_{N_{1/2}^+} + M_{N_{1/2}^+})}{2E_{N_{1/2}^+}} \gamma_5 (\bar{\alpha}_{N_{1/2}^+} p_{N_{1/2}^+}^\mu + \bar{\beta}_{N_{1/2}^+} \gamma^\mu) \\ &+ \sum_{B^-} e^{-E_B t} \lambda_{N_{1/2}^-} \gamma_5 \frac{(\gamma \cdot p_{N_{1/2}^-} + M_{N_{1/2}^-})}{2E_{N_{1/2}^-}} (\bar{\alpha}_{N_{1/2}^-} p_{N_{1/2}^-}^\mu + \bar{\beta}_{N_{1/2}^-} \gamma^\mu). \end{aligned} \quad (22)$$

These functions can then be used to relate the appropriate elements of the correlation function to a particular parity. To improve our statistics we will average the correlation functions over the spatial components of χ_3^μ .

IV. RESULTS

We begin our analysis of the spectrum by considering the 2×2 correlation matrices with χ_1 and χ_3^μ , and with χ_2 and χ_3^μ . The 2×2 correlation matrix with χ_1 and χ_2 has previously been explored in Ref. [6]. To choose a time slice at which to invert the correlation matrix, we determine the earliest plateau available to the individual interpolators. Our initial time is taken to be one time slice earlier than this. If this analysis fails, we invert the correlation matrix at one time slice earlier. This algorithm is discussed in more detail in Ref. [21]. Throughout our correlation matrix analysis we only consider a shift of one time slice from this inversion time.

Proceeding with the 2×2 correlation matrices, the eigenvectors for the projection of the χ_1 , χ_3^μ correlation matrix are obtained from an analysis at time slice $t = 14$, which is two steps back from the onset of the plateau of the effective mass extracted with χ_3^μ , and six time slices

after the source. For the χ_2 , χ_3^μ correlation matrix, the onset of the plateau in the effective mass extracted with the χ_2 interpolator is at $t = 11$. Eigenvectors for the projection of the χ_2 , χ_3^μ correlation matrix are therefore obtained from an analysis at $t = 10$.

The masses of the ground and excited states for each correlation matrix are shown in Fig. 2, along with the masses extracted with the χ_1 and χ_2 interpolators individually. In each case we find that the mass of the ground state extracted with the correlation matrix analysis is in excellent agreement with the mass of the state extracted with the χ_1 interpolator. Furthermore, the mass of the excited state extracted with the correlation matrix agrees well with the mass extracted with the χ_2 interpolator. The previous CSSM study [6] showed that the χ_1 interpolator is largely orthogonal to χ_2 . The present calculation shows, therefore, that the χ_3^μ interpolator has a significant overlap with the states accessed by both χ_1 and χ_2 .

With this information in mind we need to determine if the spin-1/2 projected χ_3^μ interpolator is a simple linear combination of χ_1 and χ_2 . Using the Fierz identity:

$$\delta_{\alpha\alpha'} \delta_{\beta\beta'} = \frac{1}{4} \sum_J (\Gamma_J)_{\alpha\beta'} (\Gamma_J^{-1})_{\beta\alpha'}, \quad (23)$$

where Γ is one of the matrices in the Dirac representation $\{1, \gamma_5, \gamma_\mu, \gamma_\mu \gamma_5, \sigma_{\mu\nu} |_{\mu > \nu}\}$, one can show that:

$$\chi_3^\mu = \frac{1}{4} \epsilon^{abc} (u^{aT} C \gamma^\sigma u^b) \gamma_\sigma \gamma^\mu d^c - \frac{1}{8} \epsilon^{abc} (u^{aT} C \sigma^{\sigma\rho} u^b) \sigma_{\sigma\rho} \gamma^\mu d^c. \quad (24)$$

Acting on χ_3^μ with the spin-1/2 projector from Ref. [7], we can write:

$$P_{\mu\nu}^{1/2} \chi_3^\nu = \frac{1}{3} \gamma_\mu \gamma_\nu \chi_3^\nu + \frac{1}{3p^2} (\gamma \cdot p \gamma_\mu p_\nu + \gamma_\nu p_\mu \gamma \cdot p) \chi_3^\nu \quad (25)$$

Expanding the combination $\gamma_\nu \chi_3^\nu$ using Eq. (24), we obtain:

$$\begin{aligned} \gamma_\nu \chi_3^\nu &= \frac{1}{4} \epsilon^{abc} (u^{aT} C \gamma^\sigma u^b) \gamma_\nu \gamma_\sigma \gamma^\nu d^c - \frac{1}{8} \epsilon^{abc} (u^{aT} C \sigma^{\sigma\rho} u^b) \gamma_\nu \sigma_{\sigma\rho} \gamma^\nu d^c \\ &= -\frac{1}{2} \epsilon^{abc} (u^{aT} C \gamma^\sigma u^b) \gamma_\sigma d^c \\ &= \frac{1}{2} \gamma_5 \chi_{SR}, \end{aligned} \quad (26)$$

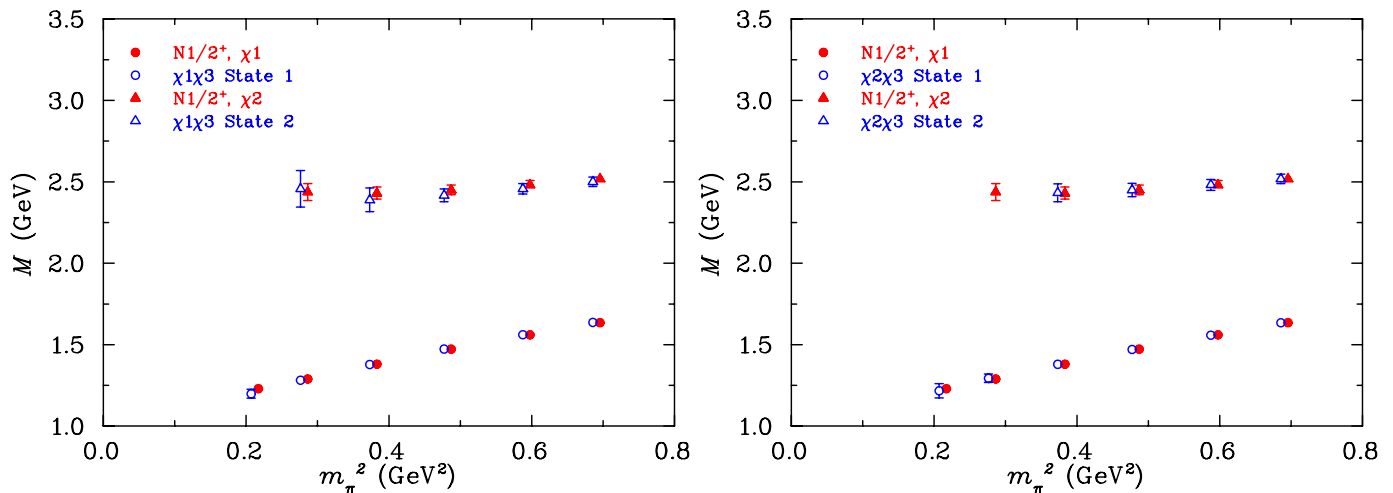


FIG. 2: Masses extracted with a 2×2 correlation matrix with χ_1 and χ_3^μ (left), and χ_2 and χ_3^μ (right). For comparison the masses extracted with the χ_1 and χ_2 interpolators are also shown. The data correspond to $m_\pi \simeq 830$ (rightmost points), 770, 700, 616, 530 and 460 MeV (leftmost points).

where we identify χ_{SR} from Ref. [5] as the linear combination $2(\chi_2 - \chi_1)$. Substituting this result in Eq. (24), we find:

$$P_{\mu\nu}^{1/2} \chi_3^\nu = \frac{1}{6} \gamma_\mu \gamma_5 \chi_{\text{SR}} + \frac{1}{3p^2} (\gamma \cdot p \gamma_\mu p_\nu + 2p_\mu p_\nu) \chi_3^\nu - \frac{1}{6p^2} (\gamma \cdot p p_\mu \gamma_5 \chi_{\text{SR}}). \quad (27)$$

At zero momentum the spin-1/2 projected χ_3^μ can then be written:

$$P_{k\nu}^{1/2} \chi_3^\nu = \frac{1}{3} \gamma_5 \gamma_k (\chi_1 - \chi_2) + \frac{1}{3} \gamma_0 \gamma_k \chi_3^0 \quad (28)$$

Since we consider the spatial components of the spin projected correlation function, $\mu = 1-3$, the only new information in the χ_3^μ interpolator is from χ_3^0 , i.e. the time component of the χ_3^μ interpolator used by Brömmel et al. [9]. Thus our analysis serves as an independent check of Ref. [9].

The Fierz transformation of the χ_3^μ interpolator allows us to verify that this has a strong overlap with both the χ_1 and χ_2 fields. The question remains whether there is sufficient additional information in the χ_3^μ interpolator to extract a second excited state. We proceed, therefore, with a 3×3 correlation matrix analysis with χ_1 , χ_2 and χ_3^μ . Eigenvectors for the projection of the correlation matrix are obtained from an analysis at $t = 10$, one step back from the onset of the plateau in the effective mass extracted with the χ_2 interpolator.

The extracted masses are shown in Fig. 3, along with the masses extracted with the χ_1 , χ_2 and χ_3^μ interpolators individually. All three determinations of the ground state mass are found to be in excellent agreement, as are the masses of the excited state extracted with the correlation matrix, and the χ_2 interpolator. At the two smaller quark masses we only have sufficient statistics to fit two of the three diagonal elements of the projected correla-

tion matrix. The masses extracted with the χ_1 and χ_2 interpolators individually are shown in Table. I.

TABLE I: The mass of the nucleon extracted with χ_1 and the even-parity spin-1/2 state excited state extracted with χ_2 . For comparison we show the mass of the even-parity spin-3/2 state extracted with χ_3 .

am_π	m_N	$m_{N'}$	$m_N^{3/2^+}$
0.541(1)	1.061(3)	1.633(14)	1.655(9)
0.501(1)	1.012(4)	1.609(18)	1.624(10)
0.454(1)	0.955(5)	1.589(21)	1.590(11)
0.401(1)	0.895(6)	1.576(25)	1.557(13)
0.347(2)	0.836(9)	1.581(34)	1.531(13)
0.302(2)	0.790(12)	...	1.515(16)
0.241(4)	0.755(13)	...	1.515(19)
0.197(5)	0.745(14)	...	1.545(26)

Our results show no evidence of a Roper-like even parity excited state, which suggests that the couplings of the interpolators used in this study to such a state must be either small or zero. On the other hand, using Bayesian techniques the analyses in Refs. [11, 12] do report a low-

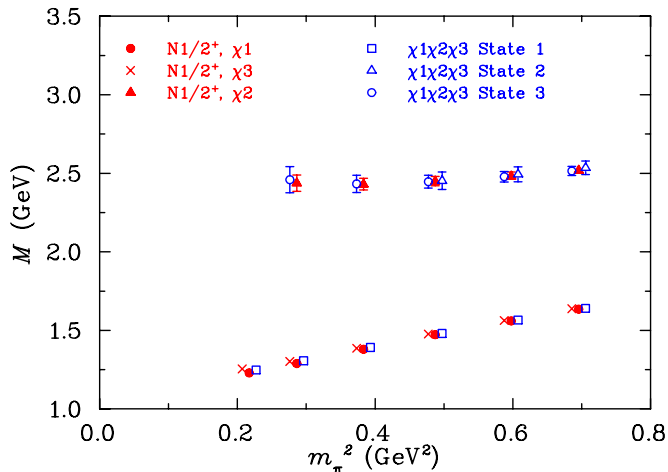


FIG. 3: As in Fig. 2, but for the 3×3 correlation matrix with the χ_1 , χ_2 and χ_3^μ interpolators.

lying state. If the Roper resonance exists in quenched QCD near its experimental value, then it would appear that our smeared sources have unfortunately poor overlap with this state. However we note that Brömmel et al. [9], Burch et al. [13], and Basak et al. [10] all report results similar to ours with different interpolating fields. It is difficult to understand, therefore, if this state does actually exist, why it would not be seen in any of these analyses.

In Fig. 4 we enlarge a portion of Fig. 1, adding the energies of the non-interacting P-wave $N + \pi$ for each study, and the mass of the even parity spin-3/2 nucleon calculated here and in Ref. [10]. We show the mass of the spin-3/2 state as a guide because it has a mass of 1720 MeV, similar to the mass of the N' . Further, at the larger quark masses it is reasonable to expect that the hyperfine splitting between the spin-1/2 and spin-3/2 states should be small. Recall that the energy of the P-wave $N + \pi$ threshold state will be larger than the attractive scattering state mass due to finite volume effects and that a stable state is likely to appear at sufficiently heavy quark masses [19, 21]. Note that for the data from Ref. [10] labeled as spin-3/2, only one of the three degenerate masses corresponds to a spin-3/2 state, with the others corresponding to higher spin states.

At the three largest quark masses, the mass of the excited state calculated in this study is consistent with the highest-lying excited state calculated by Burch et al. and with the spin-3/2 state. We also reproduce the mass of the excited state calculated by Brömmel et al. . As we approach smaller quark masses, the mass of the observed excited state becomes larger than the energy of the non-interacting P-wave $N + \pi$ state. In this case the reported masses will include some contamination from the $N\pi$ threshold, although the spectral strength may be relatively weak. Even with this low-mass contami-

nation there is no evidence of a state approaching 1440 MeV.

V. CONCLUSION

In this study we have attempted to extract the mass of the first even parity excitation of the nucleon in quenched lattice QCD, using a basis of three nucleon interpolating fields. We have demonstrated that the ground and second even parity excited states of the nucleon can be extracted from a 2×2 correlation matrix, with either the χ_1 and χ_3^μ , or χ_2 and χ_3^μ interpolating fields. With the use of the Fierz identity, we showed that the spin-1/2 projected χ_3^μ interpolator does indeed have a large overlap with the χ_1 and χ_2 interpolators, and with χ_3^0 .

Extending the analysis to a 3×3 correlation matrix, we found no evidence that our interpolators overlap with the Roper resonance. Our results are in accord with other correlation matrix based analyses using similar interpolating field constructs. The absence of a low-lying excitation in any of these analyses raises the question of how this state is seen in Bayesian analyses. Since the multiple-operator correlation matrix approach is an established method for extracting excited state masses, further careful examination of the Bayesian analyses would seem appropriate.

By comparison with the mass of the even parity spin-3/2 state at large quark masses we identify the excited state extracted in our correlation matrix as the $N'(1710)$. However we recognize that approaching the chiral regime the level ordering of the N' and the P-wave $N + \pi$ (and P-wave $N + \eta'$ in quenched QCD) is reversed. This ambiguity makes an analysis to discriminate scattering states central to future calculations of the spectrum at light quark masses.

On a final note we emphasize the need to bring these advanced analysis techniques to bare on dynamical fermion configurations. There is now ample evidence that this is likely to be the key missing ingredient in creating and observing the Roper resonance in lattice QCD simulations.

Acknowledgements

We thank the Australian Partnership for Advanced Computing (APAC) and the South Australian Partnership for Advanced Computing (SAPAC) for generous grants of supercomputer time which have enabled this project. This work was supported by the Australian Research Council. W. M. is supported by Jefferson Science Associates, LLC under U.S. DOE Contract No. DE-AC05-06OR23177. J.Z. is supported by PPARC grant PP/D000238/1.

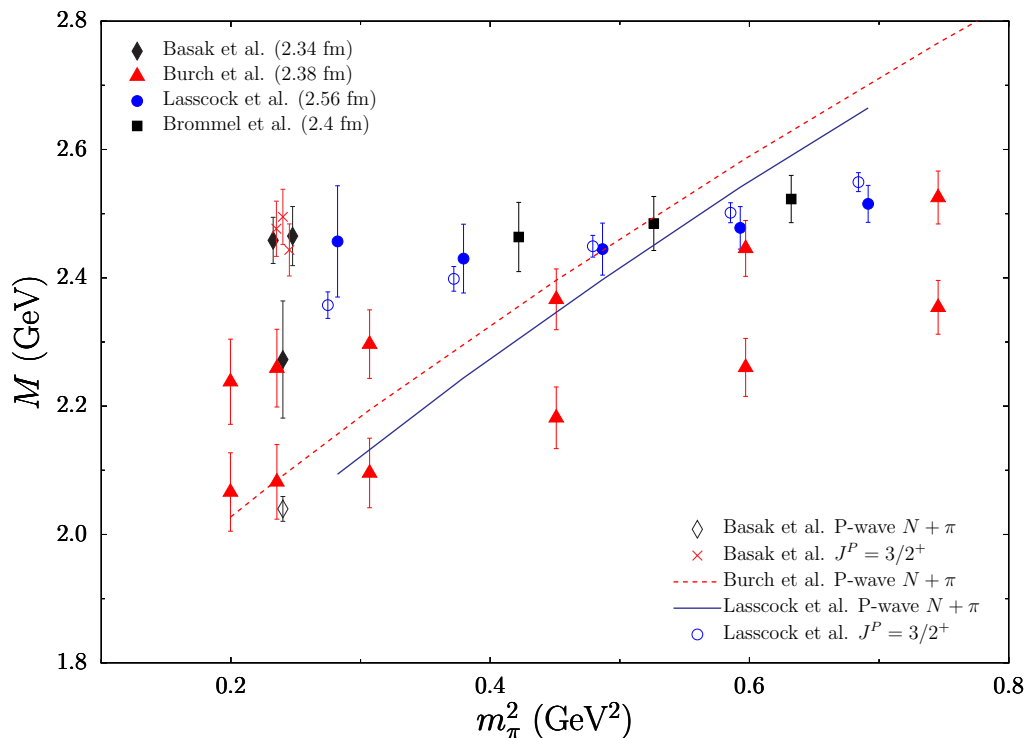


FIG. 4: A summary of existing lattice calculations of the nucleon spectrum based on correlation matrix techniques. The data points with degenerate masses from Basak et al. [10] have been displaced horizontally for clarity. P-wave two particle energies are illustrated by the two lines. The difference in the energies reflects the difference in the lattice volumes.

-
- [1] Z.-p. Li, V. Burkert, and Z.-j. Li, Phys. Rev. **D46**, 70 (1992).
- [2] C. E. Carlson and N. C. Mukhopadhyay, Phys. Rev. Lett. **67**, 3745 (1991).
- [3] O. Krehl, C. Hanhart, S. Krewald, and J. Speth, Phys. Rev. **C62**, 025207 (2000), nucl-th/9911080.
- [4] P. A. M. Guichon, Phys. Lett. **B164**, 361 (1985).
- [5] D. B. Leinweber, Phys. Rev. **D51**, 6383 (1995), nucl-th/9406001.
- [6] W. Melnitchouk et al. (CSSM Lattice Collaboration), Phys. Rev. **D67**, 114506 (2003), hep-lat/0202022.
- [7] J. M. Zanotti et al. (CSSM Lattice Collaboration), Phys. Rev. **D68**, 054506 (2003), hep-lat/0304001.
- [8] S. Sasaki, T. Blum, and S. Ohta, Phys. Rev. **D65**, 074503 (2002), hep-lat/0102010.
- [9] D. Brommel et al. (Bern-Graz-Regensburg Collaboration), Phys. Rev. **D69**, 094513 (2004), hep-ph/0307073.
- [10] S. Basak et al. (2006), hep-lat/0609052.
- [11] K. Sasaki, S. Sasaki, and T. Hatsuda, Phys. Lett. **B623**, 208 (2005), hep-lat/0504020.
- [12] N. Mathur et al., Phys. Lett. **B605**, 137 (2005), hep-ph/0306199.
- [13] T. Burch et al., Phys. Rev. **D74**, 014504 (2006), hep-lat/0604019.
- [14] T. Burch et al. (Bern-Graz-Regensburg Collaboration), Phys. Rev. **D70**, 054502 (2004), hep-lat/0405006.
- [15] S. Basak et al. (Lattice Hadron Physics Collaboration), Phys. Rev. **D72**, 074501 (2005), hep-lat/0508018.
- [16] M. Luscher and P. Weisz, Commun. Math. Phys. **97**, 59 (1985).
- [17] J. M. Zanotti et al. (CSSM Lattice Collaboration), Phys. Rev. **D65**, 074507 (2002), hep-lat/0110216.
- [18] J. M. Zanotti, B. Lasscock, D. B. Leinweber, and A. G. Williams, Phys. Rev. **D71**, 034510 (2005), hep-lat/0405015.
- [19] B. G. Lasscock et al., Phys. Rev. **D72**, 074507 (2005), hep-lat/0504015.
- [20] S. Gusken, Nucl. Phys. Proc. Suppl. **17**, 361 (1990).
- [21] B. G. Lasscock et al., Phys. Rev. **D72**, 014502 (2005), hep-lat/0503008.
- [22] F. X. Lee and D. B. Leinweber, Nucl. Phys. Proc. Suppl. **73**, 258 (1999), hep-lat/9809095.